Multi-hole pressure probes

Surrey Sensors Ltd.
Technical note TN-0616-2016, rev. 1.4

David M. Birch
May 2016

1 Introduction

Despite their comparative simplicity, multi-hole pressure probes continue to be used for the intrusive sampling of velocity components. While these sensors necessarily have a very low bandwidth (as a consequence of the length of tubing normally required to connect the probe tip to the pressure sensing elements), they have a reasonably small measurement volume (typically $\lesssim 3$ mm^3). Unlike multi-sensor hot-wire probes, however, they are temperature-insensitive and robust to the point of being nearly indestructible, and do not require frequent (time-consuming) calibration.

1.1 Principles of operation

A basic Pitot-static probe samples the local stagnation pressure P_0 at its central hole, and local static pressure P_S from holes in its side (nominally parallel to the flow). Since the probe sting may not be perfectly parallel to the flow, P_S is usually taken as the mean pressure from a number of holes arranged circumferentially around the probe body. Then, the local mean velocity parallel to the probe body U may be obtained from Bernoulli's equation, as

$$U = \left(\frac{2}{\rho} \left(P_0 - P_S \right) \right)^{1/2}, \tag{1}$$

where ρ is the fluid density, and the flow is assumed incompressible. Though (1) is formally only valid if the flow is entirely parallel to the probe axis and the probe itself is of negligible diameter, experiments have shown for a variety of Pitot-static probe tip geometries that the measured velocity is not particularly sensitive to small changes in the probe angle.

However, as the angle between the flow and the Pitot probe tip increases beyond about 10°, the pressure read by the central hole begins to decrease as the stagnation point moves too far away from the hole. While the actual pressure sampled by the hole will be a complex function of the flow angle and the probe tip geometry, for a given probe (of fixed geometry) the flow angle may be related directly to the pressure by a single function which may be obtained by calibration. Note that the effect of tip geometry upon probe effectiveness is reviewed by Chue (1975).

Consider a single tube with infinitely thin walls subjected to flow with velocity magnitude U, at some yaw angle β relative to the tube axis. If $\beta = 0°$, then the pressure P_1 sampled within the tube will be P_0 (assuming that there is no flow through the tube). Similarly, if $|\beta| = 90°$, then $P_1 = P_S$. For all angles within the range $0° < |\beta| < 90°$, then, $P_0 > P_1 > P_S$. Subtracting the static pressure from the inequality and dividing by the dynamic pressure,

$$\frac{P_0 - P_S}{\frac{1}{2}\rho U^2} > \frac{P_1 - P_S}{\frac{1}{2}\rho U^2} > 0 \tag{2}$$

Substituting Eq. (1) into the upper limit of the inequality, this reduces identically to unity and eliminates U as an independent variable. The argument, $2(P_1 - P_S)/\rho U^2$, therefore becomes a measure of the flow

angularity independent of the magnitude of the velocity, and is often defined as the coefficient of pressure C_P. Then, Eq. (2) reduces to

$$0 < C_P < 1 \tag{3}$$

and the relationship between C_P and β may be expressed as

$$\beta = f_1\left(C_P\right), \tag{4}$$

where f_1 is some continuous function defined for $0^\circ \leq |\beta| \leq 90^\circ$. The function f_1 will not be monotonic, though, since $C_P(\beta) = C_P(-\beta)$. For $\beta < -90^\circ$ or $\beta > 90^\circ$, the hole will be in the wake of the body of the tube; consequently, the measured C_P will not be meaningful, and f_1 will not necessarily be defined over this range.

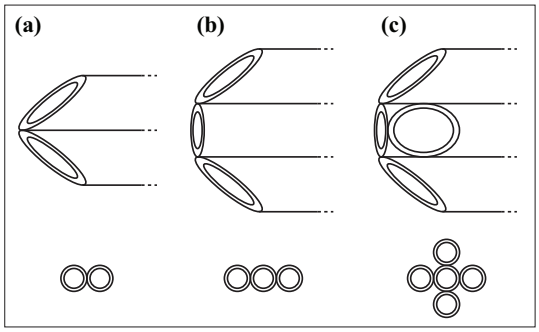

Figure 1: Geometry of common multi-hole pressure probes. (a), Two-hole yaw probe; (b) three-hole yaw-stagnation probe; (c), five-hole cruciform probe.

To extend the angular range of sensitivity, we can attach two tubes together in the shape of an 'X'. Practically, this is equivalent to joining two tubes side-by-side and cutting the ends of the tubes at an angle of 45° relative to the incoming flow (and 90° relative to each other), as illustrated in Figure 1(a). In this arrangement, one tube will be sensitive to flows between 0° and 45°, while the other tube will be sensitive to flows between −45° and 0°- and only one tube will be returning meaningful values at a time. The angle β may then be expressed piecewise, as

$$\begin{aligned} \beta &= f_1\left(C_{P1}, C_{P2}\right) \qquad -45^\circ < \beta < 0^\circ \\ \beta &= f_2\left(C_{P1}, C_{P2}\right) \qquad 0^\circ < \beta < 45^\circ, \end{aligned} \tag{5}$$

where C_{P1} and C_{P2} are the pressure coefficients measured within the two tubes, and f_1 and f_2 are arbitrary functions to be determined by calibration. This system necessarily requires *a priori* knowledge of which function to use, if a meaningful value of β is to be obtained from the set of pressure coefficients (C_{P1}, C_{P2}) at a given measurement station. To this end, it is useful to note that the tube to be used will always be the one with its face closest to being normal to the flow, and will therefore be registering the pressure coefficient closest to unity (the maximum possible value). This relationship may be used to provide an explicit definition of the ranges of the functions f_1 and f_2; (5) may equally expressed as,

$$\begin{aligned} \beta &= f_1\left(C_{P1}\right) \qquad C_{P1} > C_{P2} \\ \beta &= f_2\left(C_{P2}\right) \qquad C_{P2} > C_{P1}, \end{aligned} \tag{6}$$

Using (6), then, one may obtain the yaw angle β of an incident flow given only the two pressures coefficients (C_{P1}, C_{P2}). Obtaining the pressure coefficients from the dimensional pressures, however, also requires a measure of the local static and stagnation pressures; these are also required in order to obtain an estimate of the velocity magnitude from Eq. (1). In order to address this shortcoming, it is convenient to include a stagnation pressure tube in a yaw probe configuration, as illustrated in Figure 1(b). For relatively small angles, then, the central hole may be expected to yield a reasonable approximation of the local stagnation pressure. Although there is still no static pressure measurement directly available, the

pressure measured by the side hole *not* used in the direction measurement (and therefore reading a pressure closest to P_S) may be used as an approximation. The approximation is not a particularly good one, but the uncertainty arising from the flow angularity alone will be absorbed into f_1 and f_2.

The concept of the three-hole yaw probe may be extended into three dimensions, by combining five tubes in a cruciform arrangement; this is commonly referred to as a *five-hole probe*, and is illustrated in Figure 1(c). The calibration space of the five-hole probe may then be expressed as,

$$\begin{aligned} \alpha &= f_1(C_{P1}) \qquad C_{P1} > C_{P3} \\ \alpha &= f_3(C_{P3}) \qquad C_{P3} > C_{P1} \\ \beta &= f_2(C_{P2}) \qquad C_{P2} > C_{P4} \\ \beta &= f_4(C_{P4}) \qquad C_{P4} > C_{P2}, \end{aligned} \tag{7}$$

where α is the pitch angle and β is the yaw angle; the index '5' refers to the central hole, and the indices '1' through '4' indicate the peripheral holes, progressing counter-clockwise from the bottom.

A fundamental problem now arises: in order to obtain the pressure coefficients C_{Pi} from the measurable pressures using the definition in Eq. (**??**), the dynamic pressure $\rho U^2/2 = P_0 - P_S$ is required. However, U is one of the unknown dependent variables being measured: the problem becomes therefore becomes a circular one.

To resolve this, the stagnation pressure can be approximated by the pressure at the central hole, and the average of the pressures at the peripheral holes $\overline{P}$ can be used as an approximation of the static pressure, such that

$$\begin{aligned} P_0 &\approx P_5 \\ P_S &\approx \overline{P} = \frac{1}{4}\sum_{i=1}^{4} P_i. \end{aligned} \tag{8}$$

Then, the pressure coefficients can be redefined as

$$C_{Pi} = \frac{P_i - \overline{P}}{P_5 - \overline{P}} \tag{9}$$

Again, the redefinition of the coefficients will result in some additional uncertainty which will vary with the angle and can be absorbed into the calibration function. There may be velocity magnitude dependence in uncertainty as well- but empirical evidence suggests that this is negligible at low (incompressible) speeds.

With the coefficients and functions redefined as in Eq. (9) for convenience, Eq. (7) provides a means to relate the five pressures to the flow angularity. This is, however, a four degree-of-freedom system: the computational requirements could be significantly reduced by reducing the number of dependent variables. This can be done by observing that the difference $C_{P3} - C_{P5}$ is likely to be very sensitive to pitch but reasonably insensitive to yaw; similarly, the difference $C_{P2} - C_{P4}$ is likely to be very sensitive to yaw but reasonably insensitive to pitch. We may therefore define pitch and yaw coefficients $C_{P\alpha}$ and $C_{P\beta}$, as

$$\begin{aligned} C_{P\alpha} &= \frac{P_3 - P_1}{P_5 - \overline{P}} \\ C_{P\beta} &= \frac{P_4 - P_2}{P_5 - \overline{P}}, \end{aligned} \tag{10}$$

Equation (10) is also likely to be more sensitive to the flow angle than (7), as it is a null-centric differential measure.

Next, the velocity magnitude needs to be obtained; this can be done using Eq. (1), but the true values of P_0 and P_s must first be recovered. To do this, the difference between the approximations given in Eq. (8) and the actual values of P_0 and P_S can be mapped during the calibration. The coefficients C_{P0} and C_{PS} can be defined, such that

$$\begin{aligned} C_{P0} &= \frac{P_5 - P_0}{P_5 - \overline{P}} \\ C_{PS} &= \frac{\overline{P} - P_S}{P_5 - \overline{P}}, \end{aligned} \tag{11}$$

In practice, then, a probe is calibrated by positioning it at a series of known angles (α, β) in a flow with a fixed, known velocity magnitude U, and recording the four coefficients $(C_{P\alpha}, C_{P\beta}, C_{P0}, C_{PS})$ at each (α, β). Note that this will require that P_0 and P_S both be known during calibration- this can be achieved by positioning a Pitot-static probe near the five-hole probe during calibration. From this calibration data set, then, four independent piecewise functions f_α, f_β, f_0 and f_S may be defined, such that

$$\begin{aligned} \alpha &= f_\alpha(C_{P\alpha}, C_{P\beta}) \\ \beta &= f_\beta(C_{P\alpha}, C_{P\beta}) \\ C_{P0} &= f_0(\alpha, \beta) \\ C_{PS} &= f_S(\alpha, \beta). \end{aligned} \tag{12}$$

Then, given any set of five pressures measured in a flow of unknown angularity and magnitude, the coefficients $C_{P\alpha}$ and $C_{P\beta}$ may be determined directly from the experimental data using (10). The flow angle (α, β) may then be obtained from (12), either by interpolation or curve-fitting (see Sumner, 2002, for a comparison of these techniques). With the flow angle known, the values of C_{P0} and C_{PS} can be obtained. Then, re-arranging the definitions in (12) for $(P_0 - P_S)$ and substituting into (1),

$$|\mathbf{V}| = \left(\frac{2}{\rho} \left(P_5 - \overline{P} \right) \left(C_{PS} - C_{P0} + 1 \right) \right)^{1/2}, \tag{13}$$

where $|\mathbf{V}|$ is the magnitude of the velocity vector. It is important to note here that because the static and stagnation pressure coefficients appear in (13) as a difference only, the number of required calibration functions may be reduced by instead defining a dynamic pressure coefficient C_{Pd}, such that

$$C_{Pd} = C_{PS} - C_{P0} = \frac{P_0 - P_S}{P_5 - \overline{P}} - 1 \tag{14}$$

The coefficient C_{Pd} may then be substituted into (13). This approach may be preferable, especially if differential pressure sensors are used as it is impossible to extract absolute pressures from the process in this case.

Though inexact, this process of reducing calibration coefficients has been well documented and is generally accepted (Treaster and Yocum, 1979). This technique may be used for flow angles up to about 30°, though the error will increase with increasing flow angle.

2 Multi-hole probes

2.1 Seven-hole probes - current practice

Seven-hole pressure probes operate on much the same principle as five-hole probes, though they do tend to be somewhat different in geometry. Seven-hole probes are fairly simple to construct, as the tubes are arranged in close-packed configuration. The tip of the probe is generally machined to form a smooth cone with a fairly steep face angle (usually $60° \sim 70°$, as illustrated in Figure 2). The larger number of holes tends to result in more precise measurement, while the large face angle allows the probe to measure flows of higher angularity with reasonable precision, and provides a good means of approximating the local static pressure in flows of low angularity.

When operating at small flow angles, the seven-hole probe may be used in exactly the same way as a five-hole probe. The pitch and yaw angles are nondimensionalized into coefficients based on the differences between pressures on opposite sides of the probe, so that

$$\begin{aligned} C_{P\alpha} &= \frac{P_4 - P_1}{P_7 - \overline{P}} \\ C_{P\beta} &= \frac{P_5 + P_6 - P_2 - P_3}{2\left(P_5 - \overline{P}\right)}, \end{aligned} \tag{15}$$

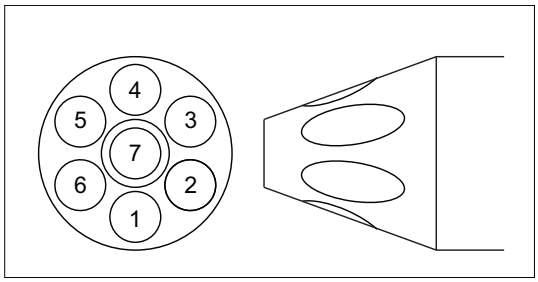

Figure 2: Typical geometry and hole numbering convention for a seven-hole pressure probe.

where the hole indices are defined as shown in Figure 2, and

$$\overline{P} = \frac{1}{6}\sum_{i=1}^{6} P_i. \tag{16}$$

Note that $C_{P\alpha}$ is identical in definition to that for the five-hole probe, while $C_{P\beta}$ differs only in that the pressures on either side of the probe tip are averaged over two holes at the same horizontal position. The static and stagnation pressure coefficients are likewise similarly defined, as

$$\begin{aligned} C_{P0} &= \frac{P_7 - P_0}{P_7 - \overline{P}} \\ C_{PS} &= \frac{\overline{P} - P_S}{P_7 - \overline{P}}, \end{aligned} \tag{17}$$

The flow angularity and velocities may be obtained from the calibration data as described in (12) and (13). As an example, Figure 3 shows typical values of $C_{P\alpha}$ and $C_{P\beta}$ for a seven-hole probe at small angles (so that the maximum pressure is recorded at hole 7).

Because of the manner in which the coefficients in (15) and (17) are defined, these coefficients are only valid if the flow remains attached everywhere on the surface of the probe tip; typically, for a conical probe tip, this restricts the flow angularity again to about 30° and corresponds to cases where the maximum pressure is recorded at the centre hole. However, for the case of high angularity (where at least half of the tip of the probe is expected to be in separated flow), a new set of coefficients may be defined.

For the case of large flow angularity (typically up to ∼60°, it is expected that the maximum pressure P_i will be recorded at some hole i, where $i \neq 7$. Because only an angular sector of the probe tip may be used, and because the probe is axisymmetric, it is more meaningful to determine the flow angularity in terms of the cone and roll angles, θ and ϕ, in a spherical coordinate system centred at the probe tip so that

$$\begin{aligned} U &= |\mathbf{V}|\cos(\alpha)\cos(\beta) &&= |\mathbf{V}|\cos(\theta) \\ V &= |\mathbf{V}|\sin(\alpha) &&= |\mathbf{V}|\sin(\theta)\sin(\phi) \\ W &= |\mathbf{V}|\cos(\alpha)\sin(\beta) &&= |\mathbf{V}|\sin(\theta)\cos(\phi), \end{aligned} \tag{18}$$

The relationship between $|\mathbf{V}|$, U, V, W, α, β, θ and ϕ is illustrated in Figure 4. Then, the cone coefficient $C_{P\theta}$ and roll coefficient $C_{P\phi}$ may be defined as

$$\begin{aligned} C_{P\theta} &= \frac{P_i - P_7}{P_i - \overline{P}} \\ C_{P\phi} &= \frac{P_{CW} - P_{CCW}}{P_i - \overline{P}}, \end{aligned} \tag{19}$$

where P_{CW} and P_{CCW} are the pressures recorded at the holes located adjacent to the ith hole in the clockwise and counter-clockwise directions, respectively. The coefficients of total and static pressure are then given in

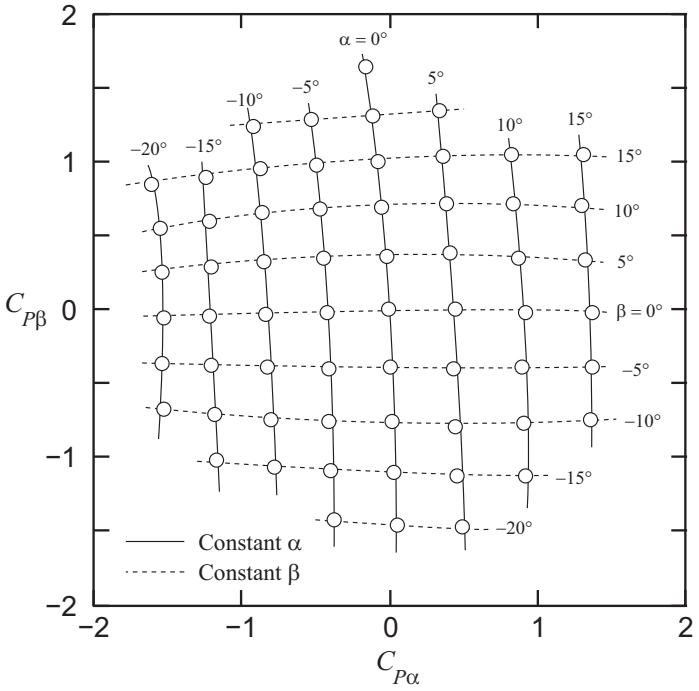

Figure 3: Coefficients of pitch and yaw for a seven-hole probe at small angles.

the same manner as (17), though recognizing that P_i now supersedes P_7 as the best available approximation of P_0, so that

$$\begin{aligned} C_{P0} &= \frac{P_i - P_0}{P_i - \overline{P}} \\ C_{PS} &= \frac{\overline{P} - P_S}{P_i - \overline{P}}. \end{aligned} \tag{20}$$

This system results in seven calibration surfaces; one low-angle case (for use when the maximum pressure is recorded at hole 7), and six high-angle cases (one for use in each of the cases where the maximum pressure is recorded at holes 1 through 6). This process for the calibration of seven-hole pressure probes is generally accepted, and is reviewed in detail by Zilliac (1989).

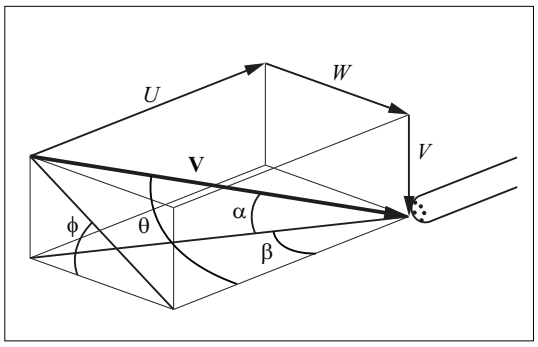

Figure 4: Graphical representation of velocities in pitch/yaw and spherical coordinate systems.

In practice, then, the probe is again calibrated by exposing it to flows at a fixed velocity magnitude U and a range of known angles (α, β). The calibration data points are then sorted into bins, depending on

which hole i is returning the highest pressure at that point, and the data in each bin used to define the calibration functions. During measurement, if the highest pressure is returned from hole 7, the data are treated similarly to the case of the five-hole probe. If, on the other hand, the highest pressure is returned at one of the peripheral holes, The calibration function obtained from that hole is used to obtain (θ, ϕ), which in turn are used to obtain $|V|$.

2.2 Generalized approaches

Dividing the calibration data into bins results in two adverse effects which can significantly increase measurement uncertainty. First, because the calibration data are sorted into bins, each calibration surface is constructed from comparatively few data points. This can decrease the fidelity of the response surface, and will amplify the uncertainty. Second, there will usually be discontinuities between the discrete calibration functions. This can lead to apparent discontinuities in measurements, and usually requires some sort of empirical blending function to minimize the resultant uncertainty.

An alternative approach is to treat the multi-hole probe data reduction problem as a more generalized problem in sensor fusion, such that

$$\begin{aligned} \alpha &= f_\alpha \left(C_{P1}, C_{P2}, ..., C_{P7} \right) \\ \beta &= f_\beta \left(C_{P1}, C_{P2}, ..., C_{P7} \right) \\ C_{Pd} &= f_d \left(\alpha, \beta \right) \end{aligned} \tag{21}$$

where the seven input parameters C_{Pi} are uncertain and have uncertainties that are functions of α and β (Shaw-Ward *et al.*, 2015, see, for example). This approach is computationally much more intensive, but is still easily within the capability of a typical desktop machine.

References

Chue, S. H. (1975). Pressure probes for fluid measurement. *Prog. Aerospace Sci.*, **36**(2), 147–223.

Shaw-Ward, S., Titchmarsh, A., and Birch, D. M. (2015). Calibration and use of n-hole velocity probes. *AIAA Journal*, **53**(2), 336–346, DoI 10.2514/1.J053130.

Sumner, D. (2002). A comparison of data-reduction methods for a seven-hole probe. *J. Fluids Eng.*, **124**, 523–527.

Treaster, A. L. and Yocum, A. M. (1979). The calibration and application of five-hole probes. *ISA Trans.*, **18**(3), 23–34.

Zilliac, G. G. (1989). Calibration of seven-hole pressure probes for use in fluid flows with large angularity. *NASA Technical Memorandum*, **102200**.